

Hexadentate Hydroxypyridonate Iron Chelators Based on TREN-Me-3,2-HOPO: Variation of Cap Size<sup>1</sup>

Jide Xu, Brendon O'Sullivan, and Kenneth N. Raymond\*

Department of Chemistry, University of California at Berkeley, California 94720-1460

Received March 21, 2002

TREN-Me-3,2-HOPO, TR322-Me-3,2-HOPO, TR332-Me-3,2-HOPO, and TRPN-Me-3,2-HOPO correspond to stepwise replacement of ethylene by propylene bridges. A series of tripodal, hexadentate hydroxypyridinone ligands are reported. These incorporate 1-methyl-3,2-hydroxypyridinone (Me-3,2-HOPO) bidentate chelating units for metal binding. They are varied by systematic enlargement of the capping scaffold which connects the binding units. The series of ligands and their iron complexes are reported. Single crystal X-ray structures are reported for the ferric complexes of all four tripodal ligands: FeTREN-Me-3,2-HOPO·0.375C<sub>4</sub>H<sub>10</sub>O·0.5CH<sub>2</sub>Cl<sub>2</sub> [*P*<sub>2</sub>/1*n* (No. 14), *Z* = 8, *a* = 20.478(3) Å, *b* = 12.353(2) Å, *c* = 27.360(3) Å;  $\beta$  = 91.60(1) $^\circ$ ]; FeTR322-Me-3,2-HOPO·CHCl<sub>3</sub>·0.5C<sub>6</sub>H<sub>14</sub>·CH<sub>3</sub>OH·0.5H<sub>2</sub>O [*P*<sub>2</sub>/1*n* (No. 14), *Z* = 4, *a* = 12.520(3) Å, *b* = 22.577(5) Å, *c* = 16.525(3) Å;  $\beta$  = 111.37(3) $^\circ$ ]; FeTR332-Me-3,2-HOPO·3.5CH<sub>3</sub>OH [*C*2/*c* (No. 15), *Z* = 8, *a* = 13.5294(3) Å, *b* = 19.7831(4) Å, *c* = 27.2439(4) Å;  $\beta$  = 101.15(3) $^\circ$ ]; FeTRPN-Me-3,2-HOPO·C<sub>3</sub>H<sub>7</sub>NO·2C<sub>4</sub>H<sub>10</sub>O [*P* $\bar{1}$  (No. 2), *Z* = 2, *a* = 11.4891(2) Å, *b* = 12.3583(2) Å, *c* = 15.0473(2) Å;  $\alpha$  = 86.857(1) $^\circ$ ,  $\beta$  = 88.414(1) $^\circ$ ,  $\gamma$  = 70.124(1) $^\circ$ ]. The structures show the importance of intermolecular hydrogen bonds and the effect of cap enlargement to the stability and geometry of the metal complexes throughout the series. All protonation and iron complex formation constants have been determined from solution thermodynamic studies. The TREN-capped derivative is the most acidic, with a cumulative protonation constant, log  $\beta_{014}$ , of 25.95. Corresponding values of 26.35, 26.93, and 27.53 were obtained for the TR322, TR332, and TRPN derivatives, respectively. The protonation constants and NMR spectroscopic data are interpreted as being due to the influence of specific hydrogen-bond interactions. The incremental enlargement of ligand size results in a decrease in iron-chelate stability, as reflected in the log  $\beta_{110}$  values of 26.8, 26.2, 26.42, and 24.48 for the TREN, TR322, TR332, and TRPN derivatives, respectively. The metal complex formation constants are also affected by the acidity of a proximal (non-metal-binding) amine in the complexes, a trend consistent with the effects of internal hydrogen bonding. The ferric complexes display reversible reduction potentials (measured relative to the normal hydrogen electrode (NHE)) between −0.170 and −0.223 V.

## Introduction

A recent in vivo evaluation of Me-3,2-HOPO ligands as iron-sequestering agents has demonstrated the superiority of a hexadentate ligand over a bidentate one.<sup>2</sup> Carboxylation of the hydroxypyridinone ring ortho to the phenolate oxygen gives a geometry which is favorable for metal-binding and

adds to chelate stability via hydrogen-bond formation.<sup>3,4</sup> The amide–phenol hydrogen bond also lowers the protonation constant of the phenolate from 8.66 for 3,2-HOPO<sup>5</sup> to 6.12 for *N*-methyl-4-propylamide-3,2-HOPO.<sup>6,7</sup> Aromaticity of the ring is enhanced, and it becomes more resistant to oxidation and reduction (e.g., *N*-methyl-3,2-HOPO is easily reduced to 3-hydroxy-2-piperidone<sup>8</sup>). Carboxylation at the desired

\* Author to whom correspondence should be addressed. Phone: (510) 642-7219. Fax: (510) 486-5283. E-mail: raymond@socrates.berkeley.edu.

- (1) Ferric Ion Sequestering Agents. 31. Part 30: Hay, B. P.; Dixon, D. A.; Vargas, R.; Garza, J.; Raymond, K. N. *Inorg. Chem.* **2001**, *40*, 3922–3935.
- (2) Yokel, R. A.; Fredenburg, A. M.; Durbin, P. W.; Xu, J. D.; Rayens, M. K.; Raymond, K. N. *J. Pharm. Sci.* **2000**, *89*, 545–555.
- (3) Raymond, K. N.; Garrett, T. M. *Pure Appl. Chem.* **1988**, *60*, 1807–1816.

- (4) Garrett, T. M.; Cass, M. E.; Raymond, K. N. *J. Coord. Chem.* **1992**, *25*, 241–253.

- (5) Raymond, K. N.; Xu, J. In *The Development of Iron Chelators for Clinical Use*; Bergeron, R. J., Brittenham, G. M., Eds.; CRC Press: Boca Raton, FL, 1994; pp 307–327.

- (6) Xu, J.; Durbin, P. W.; Kullgren, B.; Raymond, K. N. *J. Med. Chem.* **1995**, *38*, 2606–2614.

- (7) Sunderland, C. J. Ph.D. Dissertation, University of California at Berkeley, Berkeley, CA, 1998.

4-position in 3,2-hydroxypyridinone ligands may be directed by prior alkylation of the ring nitrogen.<sup>9,10</sup>

Activation as the thiazolidine of the carboxylate-derivatized hydroxypyridinone allows amide coupling with any ligand scaffold which is terminated by primary (or other sterically unhindered) amines. In the present study, this procedure is used to prepare a series of ligands in which the size of the capping scaffold is systematically increased, providing a fine tuning of the ligand structure. Earlier studies have thoroughly examined the influence of the preorganization and rigidity in a range of ligand scaffolds for catechol ligands, including the tri-lactone ring of enterobactin<sup>11</sup> the mesitylene of MECAM<sup>12</sup> and aliphatic tri-amines as in TREN-CAM.<sup>13,14</sup>

One of the compounds in this series, TREN-Me-3,2-HOPO, has been the subject of several studies for a variety of potential applications.<sup>15</sup> The further development of hexadentate hydroxypyridonate iron sequestering agents is the focus of the present study. Crystallographic, spectroscopic, thermodynamic, and electrochemical studies have been combined to illuminate the role of cap size and the effects of internal hydrogen bonding upon iron-chelate stability.

## Experimental Details

**General Synthetic Considerations.** All chemicals were obtained from commercial suppliers (Aldrich or Fisher) and were used as received. Reactions were carried out under an atmosphere of nitrogen. 3-Benzyloxy-1-methyl-2-oxo-1,2-dihydro-pyridine-4-carboxylic acid (**1**) was prepared as described previously.<sup>6</sup> Literature methods with modification were used to prepare bis(3-phthalimidopropyl)amine,<sup>16</sup> *N*<sup>1</sup>,*N*<sup>1</sup>-bis-(2-amino-ethyl)-propane-1,3-diamine,<sup>17</sup> tris(3-aminopropyl)amine (TRPN),<sup>18</sup> and *N*<sup>1</sup>,*N*<sup>1</sup>,*N*<sup>1</sup>-tris(2-acetylamidoethyl)amine.<sup>19</sup> Flash silica gel chromatography was performed using ICN 60 Å silica gel. Microanalyses were performed by the Microanalytical Services Laboratory, and mass spectra were recorded at the Mass Spectrometry Laboratory, both of the College of Chemistry, University of California, Berkeley, CA. Unless otherwise specified, all NMR spectra were recorded at ambient temperature on Bruker DRX 500, AMX 400, or AMX 300 spectrometers. Melting points were taken on a Buchi melting apparatus and are uncorrected.

**Syntheses. 3-Benzyloxy-1-methyl-2-oxo-1,2-dihydro-pyridine-4-carbonyl chloride (2).** To a slurry of compound **1** (7.53 g, 30 mmol) in benzene (30 mL) and oxalyl chloride (5.1 g, 40 mmol)

was added a drop of DMF while stirring. The mixture was heated to 60° C under N<sub>2</sub> for 3 h, and then, the solvent was removed under reduced pressure. The residue was further dried under high vacuum (0.01 mm Hg) for 4 h to give a pale yellow oil as raw product (8.1 g, raw yield 100%) and was used without further purification. <sup>1</sup>H NMR (500 MHz, CDCl<sub>3</sub>): δ = 3.52 (s, 3H, CH<sub>3</sub>); 5.42 (s, 2H, CH<sub>2</sub>Ph); 6.34 (d, 1H, *J* = 7.0 Hz, ArH); 7.05 (d, 1H, *J* = 7.0 Hz, ArH); 7.28–7.35 (m, 3H, ArH); 7.46 (d, *J* = 7.0 Hz, 2H). <sup>13</sup>C NMR (125 MHz, CDCl<sub>3</sub>): δ = 37.67, 73.9, 103.0, 128.2, 128.2, 128.6, 132.0, 132.2, 136.0, 146.8, 158.95, 163.8.

**3-Benzyloxy-1-methyl-4-(2-thioxo-thiazolidine-3-carbonyl)-1H-pyridin-2-one (3).** To a solution of **2** (8.1 g, 30 mmol) in dry methylene chloride (50 mL) was added a solution of 2-mercaptothiazoline (4.2 g, 35 mmol) and 4 mL of triethylamine in methylene chloride (50 mL) dropwise while stirring with cooling (ice bath). The reaction mixture was stirred overnight and then washed with 1 M HCl (40 mL) and 1 M KOH (40 mL) solutions, successively. The yellow organic phase was evaporated to dryness, and the residue was crystallized from 2-propanol, yielding bright yellow crystals (10.0 g, 88.8%). <sup>1</sup>H NMR (500 MHz, CDCl<sub>3</sub>): δ = 2.85 (t, 2H, *J* = 7.3 Hz, CH<sub>2</sub>), 3.53 (s, 3H, CH<sub>3</sub>), 4.26 (t, 2H, *J* = 7.0 Hz, CH<sub>2</sub>), 5.30 (s, 2H, CH<sub>2</sub>Ph); 6.06 (d, 1H, *J* = 7.0 Hz, ArH), 7.09 (d, 1H, *J* = 7.0 Hz, ArH), 7.27–7.34 (m, 3H, ArH), 7.39 (d, 2H, *J* = 7.0 Hz, ArH). <sup>13</sup>C NMR (125 MHz, CDCl<sub>3</sub>): δ = 28.8, 37.4, 54.9, 73.7, 103.6, 127.9, 128.1, 128.2, 132.5, 132.7, 137.3, 143.6, 158.7, 165.6, 200.8.

**TREN-Me-3,2-HOPOBn (4).** Compound **3** (1.28 g, 3.5 mmol) was dissolved in methylene chloride (40 mL), and neat TREN (150 μL, 1 mmol) was added. The mixture was stirred overnight until TLC showed the reaction was complete. The product solution was subjected to column chromatography on silica with methanol/methylene chloride eluent, with the product fraction giving a white foam (0.76 g, 0.87 mmol, 87%). <sup>1</sup>H NMR (500 MHz, CDCl<sub>3</sub>): δ = 2.23 (t, 6H, *J* = 6.3 Hz, CH<sub>2</sub>), 3.07 (q, 6H, *J* = 6.3 Hz, CH<sub>2</sub>), 3.59 (s, 9H, CH<sub>3</sub>), 5.28 (s, 2H, CH<sub>2</sub>Ph); 6.71 (d, 3H, *J* = 7.5 Hz, ArH), 7.10 (d, 3H, *J* = 7.0 Hz, ArH), 7.26–7.36 (m, 3H, ArH), 7.77 (t, 3H, *J* = 5.5 Hz, amideH). <sup>13</sup>C NMR (125 MHz, CDCl<sub>3</sub>): δ = 36.9, 37.5, 51.7, 74.5, 104.5, 128.5, 128.6, 128.8, 130.5, 132.0, 136.1, 146.1, 159.3, 163.1. (+) FAB-MS (*m/z*): 870.3 [MH<sup>+</sup>].

**TREN-Me-3,2-HOPO (5).** TREN-Me-3,2-HOPOBn (**4**, 0.87 g, 1 mmol) was dissolved in a mixture of acetic acid (10 mL) and hydrochloric acid (concentrated, 10 mL) in the dark under nitrogen. The reaction was stirred for 2 days, at which point the solvent was removed in vacuo. The residue was crystallized from methanol yielding a white solid (0.440 g, 0.573 mmol, 87%). <sup>1</sup>H NMR (500 MHz, D<sub>2</sub>O–NaOD): δ = 2.90 (t, 6H, *J* = 6.3 Hz, CH<sub>2</sub>), 3.45 (s, 9H, NCH<sub>3</sub>), 3.52 (t, 6H, *J* = 6.2 Hz, HNCH<sub>2</sub>), 6.56 (d, 3H, *J* = 7.2 Hz, ArH), 6.60 (d, 3H, *J* = 7.2 Hz, ArH). <sup>1</sup>H NMR (500 MHz, DMSO-*d*<sub>6</sub>): δ = 2.29 (t, 6H, *J* = 6.0 Hz, CH<sub>2</sub>), 3.07 (t, 6H, *J* = 5.8 Hz, HNCH<sub>2</sub>), 3.45 (s, 9H, NCH<sub>3</sub>), 6.45 (t, 3H, *J* = 7.2 Hz, ArH), 7.12 (d, 3H, *J* = 7.2 Hz, ArH), 8.46 (t, 3H, *J* = 5.3 Hz, amideH). <sup>13</sup>C NMR (125 MHz, D<sub>2</sub>O–NaOD): δ = 36.5, 37.3, 52.1, 106.7, 114.5, 119.3, 160.1, 164.2, 169.4. (+) FAB-MS (*m/z*): 600.3 [MH<sup>+</sup>]. Anal. Calcd (Found) for C<sub>27</sub>H<sub>33</sub>N<sub>7</sub>O<sub>9</sub>·HCl·2H<sub>2</sub>O (672.107): C, 48.25 (48.38); H, 5.70 (5.82); N, 14.58 (14.53).

**Bis(3-phthalimidoethyl)(2-phthalimidopropyl)amine (6).** This compound was synthesized according to the general literature procedure<sup>17</sup> to yield 75%. <sup>1</sup>H NMR (500 MHz, CDCl<sub>3</sub>): δ = 1.73 (qint, 2H, *J* = 7.2 Hz, CH<sub>2</sub>); 2.63 (t, 2H, *J* = 7.2 Hz, CH<sub>2</sub>); 2.78 (t, 4H, *J* = 6.6, CH<sub>2</sub>); 3.62 (t, 2H, *J* = 7.0, CH<sub>2</sub>); 3.71 (t, 4H, *J* = 6.6, CH<sub>2</sub>); 7.63–7.79 (m, 12H, ArH). <sup>13</sup>C NMR (500 MHz, CDCl<sub>3</sub>): δ = 26.4, 35.6, 35.9, 51.1, 51.5, 123.0, 132.0, 132.0, 132.1, 133.6, 133.6, 168.1, 168.2. Anal. Calcd (Found) for C<sub>31</sub>H<sub>26</sub>N<sub>4</sub>O<sub>6</sub>·

- (8) Herdeis, C.; Dimmerling, A. *Heterocycles* **1984**, *22*, 2277–2283.  
 (9) Xu, J.; Franklin, S. J.; Whisenhunt, D. W. J.; Raymond, K. N. *J. Am. Chem. Soc.* **1995**, *117*, 7245–7246.  
 (10) Raymond, K. N.; Xu, J. U.S. Patent 5 624 901, 1997.  
 (11) Meyer, M.; Telford, J. R.; Cohen, S. M.; White, D. J.; Xu, J.; Raymond, K. N. *J. Am. Chem. Soc.* **1997**, *119*, 10093–10103.  
 (12) Hou, Z.; Stack, T. D. P.; Sunderland, C. J.; Raymond, K. N. *Inorg. Chim. Acta* **1997**, *263*, 341–355.  
 (13) Rodgers, S. J.; Lee, C.-W.; Ng, C.-Y.; Raymond, K. N. *Inorg. Chem.* **1987**, *26*, 1622–1625.  
 (14) Garrett, T. M.; McMurry, T. J.; Hosseini, M. W.; Reyes, Z. E.; Hahn, F. E.; Raymond, K. N. *J. Am. Chem. Soc.* **1991**, *113*, 2965–2977.  
 (15) Turcot, I.; Stintzi, A.; Xu, J. D.; Raymond, K. N. *J. Biol. Inorg. Chem.* **2000**, *5*, 634–641.  
 (16) Fasseur, D.; Lacour, S.; Guilard, R. *Synth. Commun.* **1998**, *28*, 285–294.  
 (17) Geue, R. J.; Sargeson, A. M.; Wijesekera, R. *Aust. J. Chem.* **1993**, *46*, 1021–1040.  
 (18) Laurino, J. A.; Knapp, S.; Schugar, H. J. *Inorg. Chem.* **1978**, *17*, 2027–2028.  
 (19) Krakowiak, K. E.; Bradshaw, J. S.; Izatt, R. M. *J. Org. Chem.* **1990**, *55*, 3364–3368.

H<sub>2</sub>O (568.593): C, 65.48 (65.37); H, 4.96 (5.11); N, 9.85 (9.53). (+) FAB-MS (*m/z*): 551.2 [MH<sup>+</sup>].

**N<sup>1</sup>,N<sup>1</sup>-Bis(2-aminoethyl)propane-1,3-diamine (TR322amine·4HCl) (7).** This compound was also prepared as described<sup>17</sup> and then crystallized from 90% ethanol, yielding colorless crystals as the product (70%). <sup>1</sup>H NMR (500 MHz, CDCl<sub>3</sub>): δ = 2.09 (qint, 2H, CH<sub>2</sub>), 3.03 (t, 2H, *J* = 7.4 Hz, CH<sub>2</sub>); 3.31 (t, 2H, *J* = 8.2 Hz, CH<sub>2</sub>), 3.41 (t, 4H, *J* = 7.4 Hz, CH<sub>2</sub>), 3.52 (t, 4H, *J* = 7.5 Hz, CH<sub>2</sub>). <sup>13</sup>C NMR (500 MHz, CDCl<sub>3</sub>): δ = 21.6, 33.8, 36.3, 49.7, 50.7. Anal. Calcd (Found) for C<sub>7</sub>H<sub>20</sub>N<sub>4</sub>·4HCl·2H<sub>2</sub>O (342.16): C, 24.57 (24.26); H, 8.25 (8.42); N, 16.37 (16.11).

**TR322-Me-3,2-HOPOBn (8).** Compound **3** (1.28 g, 3.5 mmol) was dissolved in methylene chloride (40 mL), and a solution of TR322amine HCl salt (0.23 g, 1 mmol) and KOH (4 mmol) in methanol (20 mL) was added dropwise. The reaction was stirred overnight until TLC showed it was complete. The solvent was removed, leaving a pale yellow oil which was subjected to column chromatography on silica (40 mL) with methanol/methylene chloride as eluent. The desired product was obtained as white foam (0.68 g, 0.81 mmol, 81%). <sup>1</sup>H NMR (500 MHz, CDCl<sub>3</sub>): δ = 1.22 (qint, 2H, *J* = 7.1 Hz, CH<sub>2</sub>), 2.15 (t, 2H, *J* = 7.4 Hz, CH<sub>2</sub>), 2.22 (t, 4H, *J* = 6.6 Hz, CH<sub>2</sub>), 3.04 (q, 2H, *J* = 6.6 Hz, CH<sub>2</sub>), 3.11 (q, 4H, *J* = 6.2 Hz, CH<sub>2</sub>), 3.57 (s, 6H, CH<sub>3</sub>), 3.59 (s, 3H, CH<sub>3</sub>); 5.25 (s, 4H, PhCH<sub>2</sub>), 5.29 (s, 2H, PhCH<sub>2</sub>), 6.71 (d, 2H, *J* = 7.2 Hz, ArH), 6.74 (d, 1H, *J* = 7.2 Hz, ArH), 7.09 (d, 2H, *J* = 7.2 Hz, ArH), 7.10 (d, 1H, *J* = 7.2 Hz, ArH), 7.26–7.41 (m, 15H, ArH); 7.80 (t, 1H, *J* = 5.2 Hz, amideH); 7.85 (t, 1H, *J* = 5.2 Hz, amideH). <sup>13</sup>C NMR (125 MHz, CDCl<sub>3</sub>): δ = 25.5, 37.1, 37.3, 50.8, 51.7, 74.3, 74.5, 104.3, 104.5, 128.3, 128.4, 128.4, 128.5, 128.6, 128.7, 130.4, 131.9, 135.9, 136.1, 146.0, 159.2, 159.3, 162.8, 163.0. (+) FAB-MS (*m/z*): 884.5 [MH<sup>+</sup>].

**TR322-Me-3,2-HOPO (9).** TR322-Me-3,2-HOPOBn (0.63 g, 0.75 mmol) was deprotected by the same acidic deprotection procedure as TREN-Me-3,2-HOPOBn, yield 87%. <sup>1</sup>H NMR (500 MHz, D<sub>2</sub>O–NaOD): δ = 1.61 (qint, 2H, *J* = 7.5, CH<sub>2</sub>), 2.50 (t, 2H, *J* = 7.7 Hz, CH<sub>2</sub>); 2.62 (t, 4H, *J* = 6.5 Hz, CH<sub>2</sub>); 3.20 (s, br, 8H, 2CH<sub>3</sub> + CH<sub>2</sub>); 3.24 (s, 3H, CH<sub>3</sub>), 3.31 (t, 4H, *J* = 6.5 Hz, CH<sub>2</sub>), 6.25 (d, 2H, *J* = 7.0 Hz, ArH); 6.30 (d, 1H, *J* = 7.0 Hz, ArH); 6.38 (d, 2H, *J* = 7.0 Hz, ArH); 6.40 (d, 1H, *J* = 7.0 Hz, ArH). <sup>13</sup>C NMR (125 MHz, D<sub>2</sub>O–NaOD): δ = 25.4, 36.43, 37.1, 37.4, 50.9, 106.7, 114.8, 114.8, 119.8, 160.0, 160.1, 164.2, 169.4, 169.5. (+) FAB-MS (*m/z*): 614 [MH<sup>+</sup>]. Anal. Calcd (Found) for C<sub>28</sub>H<sub>35</sub>N<sub>7</sub>O<sub>9</sub>·HCl·2H<sub>2</sub>O (686.134): C, 49.01 (48.81); H, 5.87 (5.95); N, 14.29 (14.06).

**Bis(3-phthalimidopropyl)(2-phthalimidoethyl)amine (10).** Bis-(3-phthalimidopropyl)amine (10 g, 25 mmol), *N*-(2-bromoethyl)phthalimide (10 g, 40 mmol), and anhydrous Na<sub>2</sub>CO<sub>3</sub> (5 g, 47 mmol) were ground together and heated under nitrogen at 160 °C for 5 h. The reaction mixture melted and then solidified on cooling. It was ground up and partitioned in methylene chloride (100 mL) and water (100 mL). The organic phase was evaporated to half its volume and cooled to 0 °C. The product precipitated on standing and was collected by filtration, yield 8.8 g. Chromatography of the mother liquor gave an additional 2.1 g of product, total yield 77%. <sup>1</sup>H NMR (500 MHz, CDCl<sub>3</sub>): δ = 1.66 (qint, 4H, *J* = 6.9, CH<sub>2</sub>); 2.46 (t, 4H, *J* = 6.9, CH<sub>2</sub>); 2.61 (t, 2H, *J* = 6.7, CH<sub>2</sub>); 3.55 (t, 4H, *J* = 7.2, CH<sub>2</sub>); 3.63 (t, 2H, *J* = 6.7, CH<sub>2</sub>); 7.53–7.58 (m, 6H, ArH), 7.63–7.66 (m, 6H, ArH). <sup>13</sup>C NMR (500 MHz, CDCl<sub>3</sub>): δ = 25.9, 35.4, 35.7, 51.0, 51.1, 122.6, 122.7, 131.7, 131.7, 133.4, 133.4, 167.8, 167.8. Anal. Calcd (Found) for C<sub>32</sub>H<sub>28</sub>N<sub>4</sub>O<sub>6</sub>·1.5 H<sub>2</sub>O (591.61): C, 64.96 (64.67); H, 5.28 (5.34); N, 9.47 (9.35).

**N<sup>1</sup>-(2-Aminoethyl)-N<sup>1</sup>-(3-aminopropyl)-propane-1,3-diamine (TR332amine·4HCl) (11).** Compound **10** (5.6 g, 10 mmol),

KOH pellets (6.5 g, 0.1 mmol), and water (10 mL) were heated at 180 °C for 6 h in a sealed stainless steel Parr bomb. The resultant solution was acidified with HCl to pH 1 and the phthalic acid removed by filtration. The filtrate was diluted to 300 mL and loaded on a Dowex 50W-X2 (H<sup>+</sup>) column. After the column was washed with 0.5 M HCl (300 mL) and 1 M HCl (300 mL), the TR332amine HCl salt was eluted with 2 M HCl, and the eluent was evaporated to dryness, yielding a pale yellow solid. Recrystallization from 95% ethanol gave colorless crystals (2.59 g, 7.1 mmol, 71%). <sup>1</sup>H NMR (500 MHz, CDCl<sub>3</sub>): δ = 2.01–2.13 (m, 4H), 3.00 (t, 4H, *J* = 7.8, CH<sub>2</sub>); 3.29 (t, 4H, *J* = 8.4, CH<sub>2</sub>); 3.36–3.42 (m, 2H, CH<sub>2</sub>); 3.47–3.53 (m, 2H, CH<sub>2</sub>). <sup>13</sup>C NMR (500 MHz, CDCl<sub>3</sub>): δ = 22.5, 34.6, 37.3, 50.1, 51.3. Anal. Calcd (Found) for C<sub>8</sub>H<sub>22</sub>N<sub>4</sub>·4HCl·2.5H<sub>2</sub>O (365.19): C, 26.31 (26.25); H, 8.55 (8.67); N, 15.34 (15.13).

**TR332-Me-3,2-HOPOBn (12).** This compound was prepared by the same procedure as TR322-Me-3,2-HOPOBn, except the TR332amine HCl salt (0.37 g, 1 mmol) was used instead of the TR322amine HCl salt. Separation and purification were performed as described for TR322-Me-3,2-HOPOBn; pure material was obtained as white foam (0.78 g, 0.87 mmol, 87%). <sup>1</sup>H NMR (500 MHz, CDCl<sub>3</sub>): δ = 1.28 (qint, 4H, *J* = 7.1 Hz, CH<sub>2</sub>), 2.72 (t, 4H, *J* = 7.2 Hz, CH<sub>2</sub>), 2.32 (t, 2H, *J* = 6.5 Hz, CH<sub>2</sub>), 3.11 (q, 4H, *J* = 6.6 Hz), 3.19 (q, 2H, *J* = 6.2 Hz, CH<sub>2</sub>), 3.56 (s, 3H, CH<sub>3</sub>), 3.58 (s, 6H, CH<sub>3</sub>); 5.34 (ss, 4 + 2H, CH<sub>2</sub>Ph); 6.73 (d, 3H, *J* = 7.5 Hz, ArH), 7.07 (d, 3H, *J* = 8 Hz, ArH), 7.27–7.40 (m, 15H, ArH); 7.84 (t, 2H, *J* = 5.5 Hz, amideH); 7.94 (t, 1H, *J* = 5 Hz, amideH). <sup>13</sup>C NMR (125 MHz, CDCl<sub>3</sub>): δ = 26.2, 37.3, 37.5, 50.8, 52.0, 74.3, 74.5, 104.3, 104.6, 128.3, 128.4, 128.4, 128.5, 128.6, 128.7, 130.5, 130.6, 131.9, 136.0, 136.1, 146.0, 146.0, 159.3, 159.3, 162.9, 163.0. (+) FAB-MS (*m/z*): 898.5 [MH<sup>+</sup>].

**TR332-Me-3,2-HOPO (13).** TR332-Me-3,2-HOPOBn (0.67 g, 0.75 mmol) was deprotected by the same acidic deprotection procedure as TREN-Me-3,2-HOPOBn, yield 87%. <sup>1</sup>H NMR (500 MHz, D<sub>2</sub>O–NaOD): δ = 1.52 (qint, 4H, *J* = 7.5, CH<sub>2</sub>), 2.37 (t, 4H, *J* = 7.5 Hz, CH<sub>2</sub>); 2.50 (t, 2H, *J* = 7.5 Hz, CH<sub>2</sub>); 3.08 (t, 4H, *J* = 6.5, CH<sub>2</sub>); 3.10 (s, 6H, CH<sub>3</sub>), 3.11 (s, 3H, CH<sub>3</sub>), 6.20 (d, 1H, *J* = 6.5 Hz, ArH); 6.21 (d, 2H, *J* = 7 Hz, ArH); 6.33 (d, 2H, *J* = 7 Hz, ArH); 6.34 (d, 1H, *J* = 6.5 Hz, ArH). <sup>13</sup>C NMR (100 MHz, D<sub>2</sub>O–NaOD): δ = 25.4, 36.4, 37.1, 37.4, 50.9, 106.7, 114.8, 114.8, 119.8, 160.0, 164.2, 169.4, 169.5. (+) FAB-MS (*m/z*): 628 [MH<sup>+</sup>]. Anal. Calcd (Found) for C<sub>29</sub>H<sub>37</sub>N<sub>7</sub>O<sub>9</sub>·HCl·2.5H<sub>2</sub>O (709.169): C, 49.11 (49.28); H, 6.11 (6.25); N, 13.83 (13.63).

**TRPN-Me-3,2-HOPOBn (14).** This compound was prepared by the same procedure as TREN-Me-3,2-HOPOBn, with substitution of TRPN (N<sup>1</sup>, N<sup>1</sup>, N<sup>1</sup>-tris(3-aminopropyl)amine, 0.19 g, 1.0 mmol) for TREN. Separation and purification were performed as described for TREN-Me-3,2-HOPOBn; pure material was obtained as a white foam. Yield: 0.72 g, (0.83 mmol, 83%). <sup>1</sup>H NMR (500 MHz, CDCl<sub>3</sub>): δ = 1.33 (qint, 6H, *J* = 6.9 Hz, CH<sub>2</sub>), 2.14 (t, 6H, *J* = 6.9 Hz, CH<sub>2</sub>), 3.17 (q, 6H, *J* = 6.6 Hz, CH<sub>2</sub>), 3.58 (s, 9H, CH<sub>3</sub>), 5.34 (s, 6H, CH<sub>2</sub> Ph); 6.72 (d, 3H, *J* = 7.2 Hz, ArH), 7.09 (d, 3H, *J* = 7.2 Hz, ArH), 7.30–7.43 (m, 15H, ArH), 7.91 (t, 3H, *J* = 5.5 Hz, amideH). <sup>13</sup>C NMR (125 MHz, CDCl<sub>3</sub>): δ = 25.9, 37.0, 37.4, 50.4, 74.1, 104.1, 128.1, 128.3, 130.5, 131.7, 135.6, 145.4, 158.8, 162.4. FAB-MS (+): *m/z*: 912.3 [MH<sup>+</sup>].

**TRPN-Me-3,2-HOPO (15).** TRPN-Me-3,2-HOPOBn (0.65 g, 0.75 mmol) was deprotected by the same procedure as TREN-Me-3,2-HOPOBn, yield 85%. <sup>1</sup>H NMR (500 MHz, D<sub>2</sub>O–NaOD): δ = 1.26 (s, br, 6H, CH<sub>2</sub>), 2.07 (s, br, 6H, CH<sub>2</sub>), 2.81 (s, 9H, CH<sub>3</sub>), 2.85 (s, br, 6H, CH<sub>2</sub>), 5.88 (d, 3H, *J* = 7.0 Hz, ArH), 6.07 (d, 3H, *J* = 7.0 Hz, ArH). <sup>1</sup>H NMR (500 MHz, DMSO-*d*<sub>6</sub>): δ = 1.91 (s, br, 6H, CH<sub>2</sub>), 3.09 (s, br, 6H, CH<sub>2</sub>), 3.33 (q, 6H, *J* = 5.4 Hz, CH<sub>2</sub>), 3.44 (s, 9H, CH<sub>3</sub>), 6.52 (d, 3H, *J* = 7.2 Hz, ArH), 7.15 (d, 3H, *J*

**Table 1.** Crystallographic Details for Complex  $\text{FeL}^1 \cdot 0.375\text{C}_4\text{H}_{10}\text{O} \cdot 0.5\text{CH}_2\text{Cl}_2$ ,  $\text{FeL}^2 \cdot \text{CHCl}_3 \cdot \text{CH}_3\text{OH} \cdot 0.5\text{C}_6\text{H}_{14} \cdot 0.5\text{H}_2\text{O}$ ,  $\text{FeL}^3 \cdot 3.5\text{CH}_3\text{OH}$ , and  $\text{FeL}^4 \cdot \text{C}_3\text{H}_7\text{NO} \cdot \text{C}_4\text{H}_{10}\text{O}$ 

	FeTREN-Me-3,2-HOPO <sup>a</sup>	FeTR322-Me-3,2-HOPO <sup>b</sup>	FeTR332-Me-3,2-HOPO <sup>c</sup>	FeTRPN-Me-3,2-HOPO <sup>d</sup>
chem formula	$\text{FeC}_{29}\text{H}_{34.75}\text{N}_7\text{O}_{9.375}\text{Cl}$	$\text{FeC}_{33}\text{H}_{45}\text{N}_7\text{O}_{10.5}\text{Cl}_3$	$\text{FeC}_{32.5}\text{H}_{48}\text{N}_7\text{O}_{12.5}$	$\text{FeC}_{37}\text{H}_{53}\text{N}_8\text{O}_{11}$
fw (amu)	722.68	869.97	790.62	841.73
space group	$P2(1)/n$ (No. 14)	$P2(1)/n$ (No. 14)	$C2/c$ (No. 15)	$P\bar{1}$ (No. 2)
<i>a</i> , Å	20.478(3)	12.520(3)	13.5294(3)	11.4891(2)
<i>b</i> , Å	12.3531(13)	22.577(5)	19.7831(4)	12.3583(2)
<i>c</i> , Å	27.360(3)	16.525(3)	27.2439(4)	15.0473(2)
$\alpha$ , deg	90	90	90	86.8570(10)
$\beta$ , deg	91.600(10)	111.37(3)	101.15	88.4140(10)
$\gamma$ , deg	90	90	90	70.1240(10)
Z	8	4	8	2
$\rho_{\text{calcd}}$ , g/cm <sup>3</sup>	1.321	1.446	1.264	1.289
$\lambda$ , Å	0.71073	0.71073	0.71073	0.71073
$\mu$ , cm <sup>-1</sup>	4.9	6.0	4.8	5.6
<i>T</i> , °C	-116(2)	-112(2)	-130(2)	-110(2)
final <i>R</i> indices	R1 = 0.0653,	R1 = 0.0788,	R1 = 0.0735,	R1 = 0.0480,
[ <i>I</i> > 2 $\sigma$ ( <i>I</i> )] <sup>e</sup>	wR2 = 0.1222	wR2 = 0.1824	wR2 = 0.1616	wR2 = 0.1115

<sup>a</sup> For complex  $\text{FeL}^1 \cdot 0.375\text{C}_4\text{H}_{10}\text{O} \cdot 0.5\text{CH}_2\text{Cl}_2$ . <sup>b</sup>  $\text{FeL}^2 \cdot \text{CHCl}_3 \cdot \text{CH}_3\text{OH} \cdot 0.5\text{C}_6\text{H}_{14} \cdot 0.5\text{H}_2\text{O}$ . <sup>c</sup>  $\text{FeL}^3 \cdot 3.5\text{CH}_3\text{OH}$ . <sup>d</sup>  $\text{FeL}^4 \cdot \text{C}_3\text{H}_7\text{NO} \cdot \text{C}_4\text{H}_{10}\text{O}$ . <sup>e</sup>  $R1 = \sum ||F_o| - |F_c|| / \sum |F_o|$ ,  $wR2 = (\sum [w(F_o^2 - F_c^2)^2] / \sum w(F_o^2)^2)^{1/2}$ .

= 7.2 Hz, ArH), 8.62 (t, 3H, *J* = 5.4 Hz, AmideH), 10.44 (s, br, 3H, phenol H). <sup>13</sup>C NMR (125 MHz, D<sub>2</sub>O–NaOD):  $\delta$  = 25.1, 37.0, 37.2, 50.0, 106.5, 114.5, 119.5, 160.0, 164.1, 169.2. (+) FAB-MS (*m/z*): 642.3 [MH<sup>+</sup>]. Anal. Calcd (Found) for  $\text{C}_{30}\text{H}_{39}\text{N}_7\text{O}_9 \cdot \text{HCl} \cdot 2\text{H}_2\text{O}$  (713.18): C, 50.45 (50.38); H, 6.21 (6.12); N, 13.73 (13.53).

**Synthesis of Iron Complexes.** In each case, a solution of  $\text{FeCl}_3 \cdot 6\text{H}_2\text{O}$  (27 mg, 0.1 mmol) in water (5 mL) was added to a stirred solution of the appropriate ligand (0.10 mmol) in water (20 mL). The resultant purple-red solutions were neutralized with a saturated  $\text{NaHCO}_3$  solution. The complexes deposit upon standing overnight. They were filtered and dried, yielding black-red crystals. Crystals of X-ray quality were prepared by vapor diffusion methods.

**[Fe-TREN-Me-3,2-HOPO]·2H<sub>2</sub>O (17).** A 74 mg portion of the ligand was used (0.1 mmol), yielding 62 mg, 92.5%. (+) FAB-MS (*m/z*): 653.3 [MH<sup>+</sup>]. Anal. Calcd (Found) for  $\text{FeC}_{27}\text{H}_{30}\text{N}_7\text{O}_9 \cdot \text{H}_2\text{O}$ : C, 48.37 (48.36); H, 4.81 (5.01); N, 14.62 (14.38).

**[Fe-TR322-Me-3,2-HOPO]·2H<sub>2</sub>O (18).** A 69 mg portion of the ligand was used (0.1 mmol), yielding 59 mg, 85%. Anal. Calcd (Found) for  $\text{FeC}_{28}\text{H}_{32}\text{N}_7\text{O}_9 \cdot 1.5\text{H}_2\text{O}$ : C, 48.49 (48.31); H, 5.08 (5.22); N, 14.13 (13.88).

**[Fe-TR332-Me-3,2-HOPO]·H<sub>2</sub>O (19).** A 71 mg portion of the ligand was used (0.1 mmol), yielding 52 mg, 85%. Anal. Calcd (Found) for  $\text{FeC}_{29}\text{H}_{34}\text{N}_7\text{O}_9 \cdot \text{H}_2\text{O}$ : C, 49.86 (49.91); H, 5.19 (5.27); N, 14.03 (13.76).

**Fe-TRPN-Me-3,2-HOPO]·H<sub>2</sub>O (20).** A 72 mg portion of the ligand was used (0.1 mmol), yielding 55 mg, 85%. Anal. Calcd (Found) for  $\text{FeC}_{30}\text{H}_{36}\text{N}_7\text{O}_9 \cdot \text{H}_2\text{O}$ : C, 50.56 (50.22); H, 5.09 (5.17); N, 13.76 (13.58).

**X-ray Crystallography.** Crystals of  $\text{Fe}[\text{TREN-Me-3,2-HOPO}] \cdot 0.375\text{C}_4\text{H}_{10}\text{O} \cdot 0.5\text{CH}_2\text{Cl}_2$  were obtained as dark red blocks from a solution of the complex in dichloromethane diffused with diethyl ether. Crystals of  $\text{Fe}[\text{TR322-Me-3,2-HOPO}] \cdot \text{CHCl}_3 \cdot 0.5\text{C}_6\text{H}_{14} \cdot \text{CH}_3\text{OH} \cdot 0.5\text{H}_2\text{O}$  were obtained as dark red blocks from a solution of the complex in a mixture of chloroform and methanol diffused with hexane. Crystals of  $\text{Fe}[\text{TR332-Me-3,2-HOPO}] \cdot 3.5\text{CH}_3\text{OH}$  were obtained as dark red blocks from a solution of the complex in a mixture of chloroform and methanol diffused with diethyl ether. Crystals of  $\text{Fe}[\text{TRPN-Me-3,2-HOPO}] \cdot \text{C}_3\text{H}_7\text{NO} \cdot \text{C}_4\text{H}_{10}\text{O}$  were obtained as dark red blocks from a solution of the complex in wet DMF diffused with diethyl ether. Selected crystals were mounted in Paratone N oil on the ends of quartz capillaries and frozen into place under a low-temperature nitrogen stream (N<sub>2</sub>-cooling retained

during data collection). All measurements were made on a Siemens SMART/CCD X-ray diffractometer equipped with a CCD area detector and graphite-monochromator, Mo K $\alpha$  radiation ( $\lambda$  = 0.71072 Å). The intensity data to a maximum 2 $\theta$  range of 46.34° were extracted from the frames using the program SAINT<sup>20</sup> with box parameters of 1.6 × 1.6 × 0.6.

The data were corrected for Lorentz and polarization effects, and an empirical absorption correction was applied using the XPREP and SADABS<sup>21,22</sup> program. No decay correction was applied. The structures were solved by direct methods (SHELXS-86).<sup>23</sup> After most of the atoms were located, the data set was refined using the SHELXTL-97 software package.<sup>21</sup> All nondisordered non-hydrogen atoms were refined anisotropically. Hydrogen atoms were assigned to idealized positions. Crystallographic data are summarized in Table 1 and in Tables S-1 to S-12 of the Supporting Information.

**Electrochemistry.** Equipment and procedures have been described previously,<sup>24</sup> with the exception that in some experiments a Ag/AgCl reference electrode (BAS MF-2075) was substituted for the saturated calomel electrode (BAS MF-2055). In all cases, the electrochemical potentials are reported here relative to the normal hydrogen electrode (NHE) following calibration of the reference electrodes against K<sub>4</sub>Fe(CN)<sub>6</sub> as described previously.

Aqueous solutions of the ferric-hydroxypyridinone complexes were prepared at 5 × 10<sup>-5</sup> M Fe, with ligand concentrations between 1 × 10<sup>-4</sup> and 1.4 × 10<sup>-4</sup> M with 0.01 M ammonium acetate present as pH buffer. Additions of KOH or HCl were added to give the desired pH, and the ionic strength was set to 0.1 M with KCl. Reduction potentials were determined by square wave voltammetry as described previously. Reversibility was evaluated by comparing the digitized current–potential response to the theoretical response as described in the literature.<sup>25</sup> According to eq 1, a plot of the function  $\Gamma$  against potential, *E*, has an inverse

(20) SAINT SAX Area-Detector Integration Program, version 4.024; Siemens Industrial Automation, Inc.: Madison, WI, 1994.

(21) SHELXTL Crystal Structure Analysis Determination Package, version 5.10; Siemens Analytical X-ray Systems Inc.: Madison, WI, 1997.

(22) SMART Area-Detector Software Package; Siemens Industrial Automation, Inc., Madison, 1994.

(23) Sheldrick, G. M. *Acta Crystallogr., Sect. A* **1990**, *46*, 467–473.

(24) Cohen, S. M.; O'Sullivan, B.; Raymond, K. N. *Inorg. Chem.* **2000**, *39*, 4339–4346.

(25) Aoki, K.; Maeda, K.; Osteryoung, J. J. *Electroanal. Chem.* **1989**, *272*, 17–28.

**Table 2.** Iron Formation Constants for the 3-Hydroxy-2(1*H*)-pyridinone Ligands

species	TREN-Me-3,2-HOPO			TR322- Me-3,2-HOPO		TRPN-Me-3,2-HOPO	
		potentiometric	NMR <sup>a</sup>	potentiometric	potentiometric	potentiometric	NMR <sup>a</sup>
[LH] <sup>2-</sup>	log <i>K</i> <sub>a</sub> <sup>1</sup>	8.19(2)	7.8	8.37(1)	8.94(1)	9.43(4)	9.1
[LH <sub>2</sub> ] <sup>-</sup>	log <i>K</i> <sub>a</sub> <sup>2</sup>	6.97(1)	6.8	6.99(1)	6.77(1)	6.71(3)	7.2
[LH <sub>3</sub> ] <sup>0</sup>	log <i>K</i> <sub>a</sub> <sup>3</sup>	5.83(1)	5.9	5.93(1)	6.04(1)	6.02(3)	6.4
[LH <sub>4</sub> ] <sup>+</sup>	log <i>K</i> <sub>a</sub> <sup>4</sup>	4.97(1)	4.9	5.06(1)	5.18(2)	5.37(3)	5.4
[FeL] <sup>0</sup>	log β <sub>110</sub>	26.8(1)		26.2(2)	26.42(1)	24.48(1)	
[FeLH] <sup>+</sup>	log β <sub>111</sub>	30.7(3)		30.8(1)	32.72(1)	32.2(6)	
	log <i>K</i> <sub>a</sub> <sup>FeLH</sup>	3.9		4.6	6.3	7.72	
pM(Fe <sup>III</sup> )		26.8		26.6	25.8	23.8	

<sup>a</sup> From NMR titration data, single determination only, all other constants derived from at least three independent investigations. Figures in parentheses give the uncertainty determined from the standard deviation between titrations, expressed in units of the least significant figure. pM values indicate the negative logarithm of the free iron(III) concentration calculated for the conditions of pH 7.4 and total iron and ligand concentrations of  $1 \times 10^{-6}$  and  $1 \times 10^{-5}$  M, respectively.

slope of  $2.3RT/nF$  ( $59/n$  mV) and a horizontal intercept at  $E = E^\circ$ . Terms are defined as follows: cosh is the hyperbolic cosine function,  $E_{sw}$  is the square wave modulation amplitude,  $\Delta I$  is the square wave difference current,  $\Delta I_p$  is the maximum (peak) in difference current. and the physical constants  $n$ ,  $F$ ,  $R$ , and  $T$  hold their usual meanings in an electrochemical context.

$$\Gamma = \log[z \pm (z^2 - 1)^{1/2}] = \frac{nF}{2.3RT}(E - E^\circ);$$

$$z = \left(\frac{\Delta I_p}{\Delta I}\right) \left(1 + \cosh\left(\frac{nF}{RT}E_{sw}\right)\right) - \cosh\left(\frac{nF}{RT}E_{sw}\right) \quad (1)$$

The sign is negative for  $E < E^\circ$  and positive for  $E \geq E^\circ$ .

Each of the electrochemical reduction potentials ( $E^\circ$  values) reported in Table 3 is the average of many voltammetric scans: 63, 56, 70, and 49 for the ferric complexes of TREN-, TR322-, TR332-, and TRPN-Me-3,2-HOPO, respectively. These scans were collected over the pH ranges as indicated in Table 3. Within these ranges, the observed  $E^\circ$  values met the reversibility criterion given here and were independent of pH, and the neutral complex, [FeL]<sup>0</sup>, was the only significant coordination species formed in solution. The  $E^\circ$  values were used to calculate ferrous ion formation constants (Table 3) using a standard Gibbs-cycle analysis.<sup>26,27</sup> Complexation of ferrous iron was considered to be thermodynamically equivalent to the following cycle: oxidation to the ferric state,<sup>28</sup> complexation with the appropriate hydroxypyridinone, and then reduction to the ferrous complex.

**Solution Thermodynamics.** Complex formation constants were determined using procedures and equipment closely following previous descriptions.<sup>24,29</sup>

**Solutions.** Base (0.1 M KOH), acid (0.1 M HCl), and electrolyte (0.1 M KCl) solutions were stored under a positive pressure of argon gas in order to reduce the ingress of CO<sub>2</sub> from the atmosphere. A stock solution of iron was prepared by dissolution of Fe(NO<sub>3</sub>)<sub>3</sub> (Aldrich, 99.99+%, nonahydrate) in a standard (~0.1 M) HCl solution and standardized by titration against a stock solution of EDTA (di-sodium EDTA, biochemika grade, Fluka) using a literature method<sup>30</sup> adapted as previously described.

**Titration Equipment.** The custom-built spectrophotometric titration cell was held under a positive pressure of argon to eliminate the ingress of CO<sub>2</sub> and kept at  $25 \pm 0.1$  °C. Fully automated instrumentation was used for titrant delivery and the collection of potentiometric and/or spectrophotometric data under computer control. This instrumentation was composed of Metrohm autoburets (Titrino 702 SM or Dosimat 665), either an Accumet pH meter (model AR15 or 15) or the Metrohm Titrino for electrode potential measurement, and a Hewlett-Packard 8452a spectrophotometer (diode array). A glass bulb electrode was used for the measurement

of pH (Corning high performance, combination reference electrode, cat. no. 476146). This was calibrated against proton *concentration* as opposed to *activity*, using the computer program GLEE as described previously.<sup>29,31</sup> The parameters  $E^\circ$ ,  $s$ , and  $\gamma$  were refined while a fixed value of 13.78 was used for  $pK_w$ .<sup>32,33</sup>

**Titration.** These were assembled from the constituent reagents at concentrations determined by prior modeling using estimated formation constants and the computer program HYSS.<sup>34,35</sup> The resulting solutions typically had an initial pH of ~3.5 and were incrementally perturbed by addition of titrant (either HCl or KOH) with data collection following a delay to allow for equilibration (90 s for protonation studies, 3 min for iron-hydroxypyridinone titrations, extended to 2 h for the competition experiments). All titrations were reversed; that is, titration occurred first with KOH to higher pH and then back to the initial pH with HCl. All absorbance measurements were less than 1.0 absorbance units.

**Protonation Constants.** The protonation constants of the hydroxypyridinone ligands were determined in potentiometric experiments; that is, no spectral data were collected. Concentrations between  $4 \times 10^{-4}$  and  $2 \times 10^{-3}$  M were used, and the average number of points collected in each titration was 113, collected over the pH range 4–10. Following the data analysis described later, the constants given in Table 2 were obtained with global  $\Sigma$  values between 0.92 and 3.9 (average  $\Sigma = 2.5$ ). Identical methods were used for Ac<sub>3</sub>TREN; a value of log *K*<sub>a</sub> = 6.01(1) was obtained from the analysis of 6 titrations (210 data points) with global fitting values ( $\Sigma$ ) between 0.95 and 2.1. In the course of the potentiometric analysis, an excess ( $1.55 \pm 0.05$ ) of proton equivalents were found relative to the concentration of the amine in agreement with the elemental analysis (1.6 equiv of HCl).

- (26) Stumm, W.; Morgan, J. J. *Aquatic Chemistry: an introduction emphasizing chemical equilibria in natural waters*; Wiley: New York, 1981.
- (27) Snoeyink, V. L.; Jenkins, D. *Water Chemistry*; Wiley: New York, 1980.
- (28) Huesler, K. E.; Lorenz, W. J. In *Standard potentials in aqueous solution*; Bard, A. J., Parsons, R., Jordan, J., Eds.; Marcel Dekker: New York, 1985; pp 391–412.
- (29) Johnson, A. R.; O'Sullivan, B.; Raymond, K. N. *Inorg. Chem.* **2000**, *39*, 2652–2660.
- (30) Ueno, K.; Imamura, T.; Cheng, K. L. *Handbook of organic analytical reagents*, 2nd ed.; CRC Press: Boca Raton, FL, 1992.
- (31) Gans, P.; O'Sullivan, B. *Talanta* **2000**, *51*, 33–37.
- (32) Hamed, H. S.; Owen, B. B. *The physical chemistry of electrolytic solutions*, 3rd ed.; Reinhold Publishing Corp.: New York, 1958.
- (33) Sweeton, F. H.; Mesmer, R. E.; Baes, C. F. J. *J. Solution Chem.* **1974**, *3*, 191.
- (34) Alderighi, L.; Gans, P.; Ienco, A.; Peters, D.; Sabatini, A.; Vacca, A. *Coord. Chem. Rev.* **1999**, *184*, 311–318.
- (35) Alderighi, L.; Gans, P.; Ienco, A.; Peters, D.; Sabatini, A.; Vacca, A. *HYSS*, version 2; Leeds, U.K. and Florence, Italy, 1999.

**Table 3.** Electrochemical Data for the 3-Hydroxy-2(1*H*)-pyridinone Ligands<sup>a</sup>

	TREN-Me-3,2-HOPO	TR322-Me-3,2-HOPO	TR332-Me-3,2-HOPO	TRPN-Me-3,2-HOPO
<i>E</i> <sup>o</sup> (V vs NHE)	-0.177 (6)	-0.223 (4)	-0.170 (3)	-0.185 (9)
reversible pH range	7.5–10.0	8.0–10.3	8.2–10.3	8.1–9.1
log β <sub>110</sub> [Fe <sup>II</sup> L] <sup>+</sup>	10.8 (2)	9.4 (3)	10.5 (1)	8.3 (2)

<sup>a</sup> Figures in parentheses give the uncertainty in the least significant figure, determined from the standard deviation between electrochemical measurements.

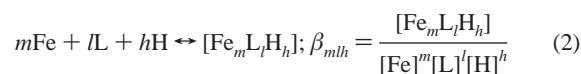
**Iron Complexation Constants.** Each experiment consisted of two titrations (forward vs KOH and reverse vs HCl). The concentration of the components was varied over the following ranges: EDTA  $2 \times 10^{-4}$  to  $1 \times 10^{-3}$  M, iron  $5 \times 10^{-5}$  to  $1 \times 10^{-4}$  M, and hydroxypyridinone ligand  $1 \times 10^{-4}$  to  $6 \times 10^{-4}$  M. In all cases, the hydroxypyridinone ligand and EDTA were both present at greater than a 10% excess over the iron concentration. For each experiment, ~24 points were collected over a 48 h period (an equilibration time of 2 h was used for each point, 12 points collected in each direction). Each data point consisted of a potentiometric measurement (pH) and an absorbance spectrum. A selection of ~80 wavelengths within the range 410–650 nm were taken from the spectral data and incorporated into the refinements, giving a matrix of ~960 absorbance measurements for each experiment. The formation constants given in Table 2 were obtained following data analysis as described later. Global Σ values were in the range 0.8–3.4 (average Σ = 2.1).

The formation constants β<sub>110</sub> and β<sub>111</sub> were simultaneously determined in the course of the competition experiments because there was significant formation of both protonation states of the ferric-hydroxypyridinone complexes, [FeL]<sup>0</sup> and [FeLH]<sup>+</sup>, in the presence of ferric-EDTA. This was true for the ligands TREN, TR322, and TR332, as illustrated for a typical experiment in Figure S-1, Supporting Information. The concurrent presence of both protonation states of the iron-hydroxypyridinone complexes may have been an artifact of the numerical fitting process because the spectral differences were minor. Therefore, the existence of the two protonation states, [FeL]<sup>0</sup> and [FeLH]<sup>+</sup>, was verified by performing a single spectrophotometric titration for each iron-hydroxypyridinone system in the absence of EDTA, allowing the acidity of each complex (i.e., the difference between β<sub>110</sub> and β<sub>111</sub>) to be verified. The value of β<sub>111</sub> was held fixed at that determined in the competition experiments while β<sub>110</sub> was refined. In all cases, the formation constants and absorbance spectra were in good agreement with those determined in the course of the competition experiments.

To evaluate the attainment of equilibrium in the competition experiments, a single batch titration was performed for the iron/TREN-Me-3,2-HOPO system. For this, a stock solution containing iron ( $5 \times 10^{-5}$  M), EDTA ( $2 \times 10^{-4}$  M), and TREN-Me-3,2-HOPO ( $1 \times 10^{-4}$  M) was prepared at pH ~ 3. Aliquots (12) were withdrawn with a calibrated, analytical grade pipet, raised in pH by an addition of KOH (up to pH 5.5), and equilibrated in sealed flasks away from light at 25 °C for one week. After this time, absorbance and pH measurements were collected for each solution and analyzed by nonlinear least-squares (vide infra), yielding formation constants, log β<sub>111</sub> = 30.34 and log β<sub>110</sub> = 26.73 (global Σ = 3.4), in agreement with the values presented in Table 2 and suggesting that the dynamic titrations accurately represent the equilibrium state.

**Data Treatment.** The data from each titration were treated by nonlinear least-squares refinement using the program HYPER-

QUAD.<sup>36,37</sup> All equilibrium constants were defined as cumulative formation constants, β<sub>*m*lh</sub> according to eq 2; the hydroxypyridinone ligands are designated as L. Stepwise protonation constants, K<sub>a</sub><sup>*n*</sup>, may be derived from these cumulative constants according to eq 3 (describes proton association constants). In the case of the competition experiments, the equilibration of iron between the hydroxypyridinone and EDTA was calculated by including the proton association and iron formation constants for EDTA as fixed parameters in the refinements (the actual values used are tabulated in Table S-13 of the Supporting Information).<sup>38,39</sup> Because of the hexacoordinate nature of both ligands, it was assumed that ternary (i.e., mixed EDTA-Fe-hydroxypyridinone) complexes were not formed. This assumption was supported by spectral data showing that the band shapes and λ<sub>max</sub> values of the LMCT transitions of the iron-hydroxypyridinone complexes were unchanged in the presence and absence of EDTA. The ferric-ion hydrolysis constants<sup>40</sup> were also incorporated as fixed parameters; in all cases, these species constituted much less than 1% of the total iron distribution. A typical analysis of a competition titration included ~20 equilibrium constants (protonation and Fe constants for the hydroxypyridinone ligand and for EDTA, Fe hydrolysis constants, and K<sub>w</sub>). Despite this complexity, the refinements were stable because only two constants were refined (β<sub>110</sub> and β<sub>111</sub>).



$$K_a^n = \frac{[\text{LH}_n]}{[\text{H}][\text{LH}_{n-1}]} = \frac{\beta_{01n}}{\beta_{01(n-1)}} \quad (3)$$

The program HYPERQUAD allows treatment of potentiometric and/or spectrophotometric data and the simultaneous treatment of multiple titration curves. An important consideration when treating data acquired from different measurement techniques (i.e., absorbance and potentiometric measurements) is the relative weighting of each observation in the refinements. For potentiometric observations, the errors are assigned as 0.002 mV and 0.002 pH. For absorbance measurements the error terms were determined using a holmium oxide glass filter as directed by the program HYPERQUAD.

Each pair of titrations (i.e., forward titration against KOH and reverse titration against HCl) were combined for simultaneous refinement. For spectral titrations, only the complexes [FeL]<sup>0</sup> and [FeLH]<sup>+</sup> were considered to have significant absorbance. For the protonation studies, both the total proton and ligand concentrations were refined, only the proton concentration was allowed to vary in the metal complexation studies, and all other concentrations were held at estimated values determined from the volume of standardized stock or the weight of ligand taken (measured to 0.01 mg). Refined concentrations were within 5% of the expected values.

**pD-NMR Titrations.** Ligand solutions in D<sub>2</sub>O were prepared and titrated by addition of ca. 10% diluted NaOD (Aldrich, 40 wt %, >99% D) in D<sub>2</sub>O. Combination glass electrodes (either Orion

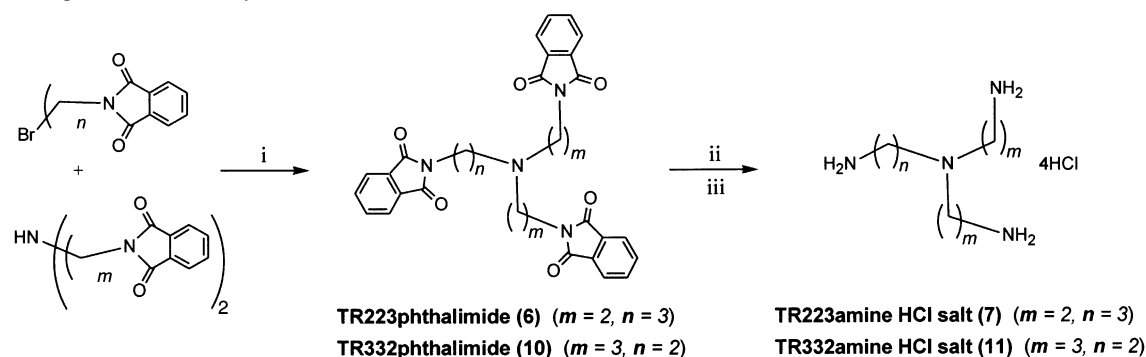
(36) Gans, P.; Sabatini, A.; Vacca, A. *HYPERQUAD2000*, <http://www.chim1.unifi.it/group/vacsab/hq2000.htm>; Leeds, U.K. and Florence, Italy.

(37) Gans, P.; Sabatini, A.; Vacca, A. *Ann. Chim. (Rome)* **1999**, *89*, 45–49.

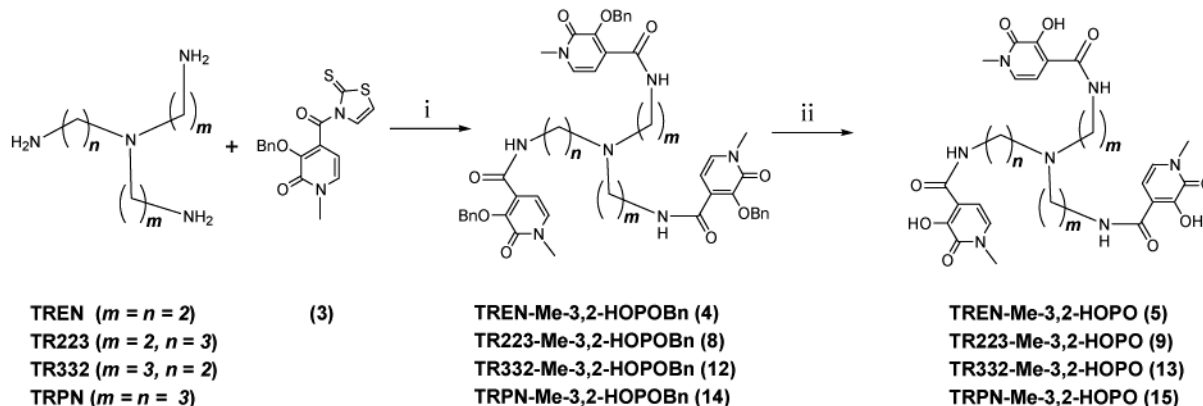
(38) Anderegg, G. *Critical Survey of Stability Constants of EDTA Complexes*; IUPAC Chemical Data Series, Pergamon Press: New York, 1977, 14.

(39) Schwarzenbach, G.; Heller, J. *Helv. Chim. Acta* **1951**, *34*, 576.

(40) Baes, C. F.; Mesmer, R. E. *The hydrolysis of cations*; Wiley: New York, 1976.

**Scheme 1.** Preparation of the Nonsymmetric Amines TR322amine (7) and TR332amine (11)<sup>a</sup>

<sup>a</sup> (i) Heating (200 °C). (ii) Concentrated NaOH solution, heating at 180 °C for 6 h in a Parr bomb. (iii) Concentrated HCl, followed by cation exchange column.

**Scheme 2.** Syntheses of Tripodal Hexadentate Me-3,2-HOPO Ligands<sup>a</sup>

<sup>a</sup> (i) Amide coupling. (ii) Catalytic hydrogenation deprotection.

semi-micro or Corning cat. no. 476146, both filled with 3 M KCl in water) were used to monitor pD. The electrodes were calibrated in the standard manner<sup>29,31</sup> by a strong acid/strong base titration in water with values of pD in the ligand titration being calculated according to the relationship  $pD = 0.4 + pH$ .<sup>41</sup> NMR spectra were recorded on Bruker spectrometers (AMX 300 or DRX 500), and chemical shifts were referenced to a solvent peak from acetonitrile (added at 0.1% v/v,  $\delta = 1.95$  ppm). Protonation constants were determined by nonlinear least-squares refinement using the program HypNMR<sup>42</sup> using an estimated uncertainty in chemical shift of 0.01 ppm (based on variation between duplicate spectra). Global fitting parameters ( $\Sigma$ ) of 1.02 and 1.55 were obtained in the course of the analysis. After the refinement, the constants were corrected for the deuterium effect according to the correlation by Delgado et al.:<sup>43</sup>  $\log K^D = 0.32 + 1.044 \log K^H$ .

## Results

**Ligand Synthesis.** Preparation of the nonsymmetric amine scaffolds (TR322 and TR332) is illustrated in Scheme 1. Syntheses of TR322phthalimide (compound 6) and the TR322amine·HCl salt (compound 7) have been reported

previously,<sup>17</sup> although full characterization and detailed preparation are given here for the first time.

Me-3,2-HOPOBn-thiazolide (3) is a versatile compound for synthesizing multidentate Me-3,2-HOPO ligands. Previously, it was prepared by the reaction of 1 with 2-mercaptothiazoline in the presence of DCC (dicyclohexyl carbodiimide) and DMAP (1,4-dimethylamino)pyridine.<sup>6</sup> We report here an improved synthetic route with higher yield. Compound 1 is converted to its acid chloride 2, which is then converted to 3. The acid chloride, 2, is a very active species; it reacts with not only aliphatic primary and secondary amines but also with aromatic amines, to form amides. The thiazolide derivative, compound 3, selectively reacts with aliphatic primary amines to form the corresponding amides. This synthetic flexibility allows the benzyl-protected hydroxypyridinone to be attached to a wide variety of amine-terminated molecular scaffolds such as the series of TREN derivatives of the current study. Scheme 2 illustrates the coupling procedure used to attach the hydroxypyridinone binding units to the amine-terminated scaffolds.

**NOE Spectroscopy of TREN-Me-3,2-HOPO.** The conformation of the HCl salt of TREN-Me-3,2-HOPO in protic ( $CD_3COOD$ ,  $D_2O$ ) and aprotic ( $DMSO-d_6$ ) solvents was investigated. Cross-peaks were observed in  $CD_3COOD$  between the hydroxypyridinone ring protons and the aliphatic TREN-backbone protons (Supporting Information Figure S-2,

(41) Perrin, D. D.; Dempsey, B. *Buffers for pH and Metal Ion Control*; Chapman and Hall Ltd.: London, 1974.

(42) Alderighi, L.; Bianchi, A.; Biondi, L.; Calabi, L.; De Miranda, M.; Gans, P.; Ghelli, S.; Losi, P.; Paleari, L.; Sabatini, A.; Vacca, A. *J. Chem. Soc., Perkin. Trans. 2* **1999**, 2741–2745.

(43) Delgado, R.; Frausto Da Silva, J. J. R.; Amorim, M. T. S.; Cabral, M. F.; Chaves, S. J. *Anal. Chim. Acta* **1991**, 245, 271.

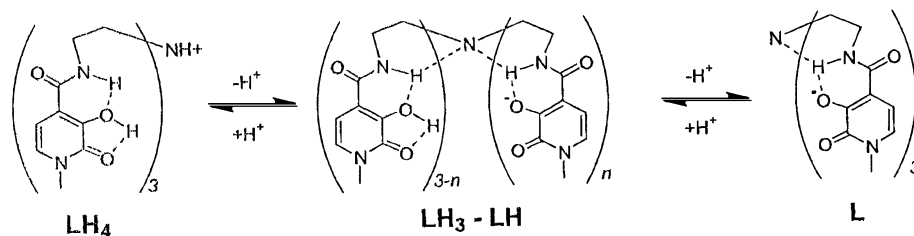


**Figure 1.** Proposed hydrogen-bonding scheme in TREN-Me-3,2-HOPO and relationship to the protonation reactions.

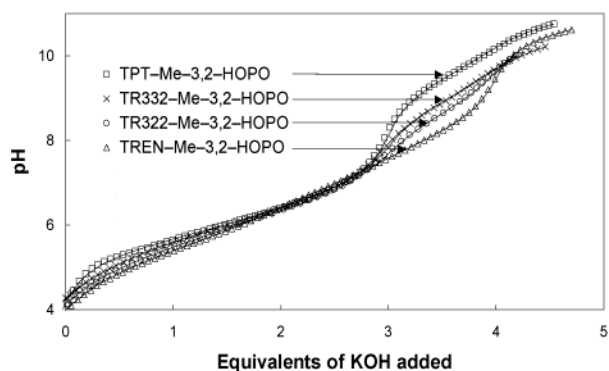


**Figure 2.** Potentiometric titration curves for the hydroxypyridinone ligands. Symbols give observed pH measurements, and lines give the calculated fits.

top diagram). These cross-peaks suggest that in the protonated form the aliphatic cap protons interact with the hydroxypyridinone ring and the *N*-methyl protons. In contrast, in an aprotic solvent (DMSO- $d_6$ ), cross-peaks were observed between the *N*-methyl group and a proximal proton (in position 6 of the ring), between this proton and the other ring proton at position 5, and finally between this latter proton and the amide proton (as shown in the Supporting Information, Figure S-2, bottom diagram). No interaction between the aliphatic cap protons and the aromatic protons was observed, suggesting that the aromatic protons are directed out toward the bulk solvent in DMSO- $d_6$  while the hydrophilic oxo and hydroxyl groups are directed into the center of the ligand. Evidence of the structural formula of  $LH_4$  and the left part of  $LH_3-LH$  in Figure 1 is that the crystal structure of 3-hydroxy-1-methyl-2-oxo-1,2-dihydro-pyridine-4-carboxylic acid propylamide (PR-Me-3,2-HOPO)<sup>44</sup> is identical to  $LH_4$  and the left part of the  $LH_3-LH$  structure, and the crystal structures of all iron complexes of Me-3,2-HOPO ligands support this structure assignment.

**Protonation Constants.** These were determined by potentiometric titration. The relatively high ligand concentrations required to ensure precise pH buffering precluded the simultaneous collection of spectral data. Figure 2 indicates the close agreement obtained between experimental observations and the numerical analysis. The constants reported for TREN-Me-3,2-HOPO (Table 2) agree within experimental uncertainty with previously reported values.<sup>9,45</sup>

The tris-acetylamine derivative  $Ac_3TREN$  was used as a model for the capping amine in the ligand TREN-Me-3,2-

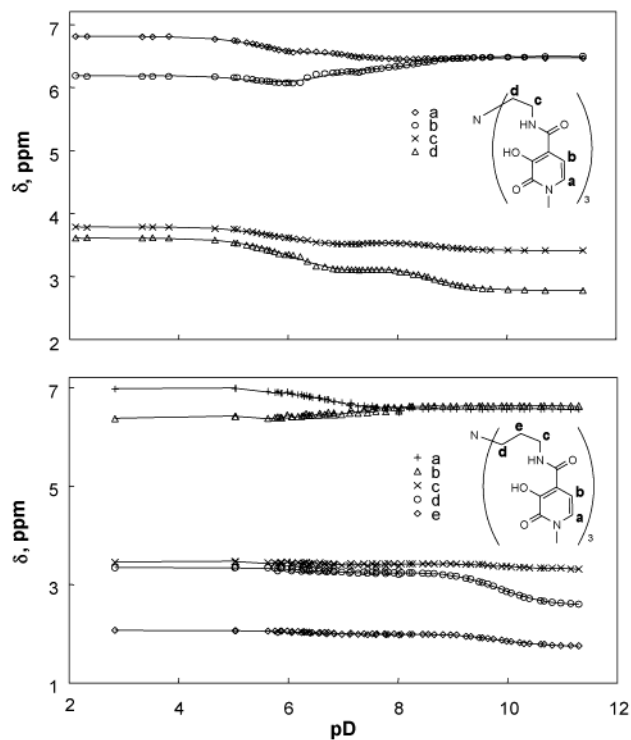


**Figure 3.** pD-NMR titration curves for the ligands TREN-Me-3,2-HOPO (top) and TRPN-Me-3,2-HOPO (bottom). Symbols give observed measurements and lines give the calculated fits.

HOPO: it shows the effect of a  $\gamma$  amide proton on the central amine basicity. A value of  $\log K_a = 6.01$  was obtained, in agreement with a previous determination.<sup>45</sup>

**pD-NMR Titrations.** Proton NMR spectra were recorded as a function of pD for the ligands at the extremes of the series, that is, TREN- and TRPN-Me-3,2-HOPO. Individual resonances in the spectra of TREN-Me-3,2-HOPO were assigned by two-dimensional  $^1H$  NMR (NOE spectrum given in Figure S-2 of the Supporting Information), and by analogy, these assignments were extended to the TRPN-Me-3,2-HOPO spectra. As shown in Figure 3, the chemical shifts of these resonances displayed sigmoidal shifts as a function of pD, which were consistent with the deprotonation reactions of the ligands. Numerical analysis of the data confirmed this relationship and yielded protonation constants in acceptable agreement with those determined by potentiometry (Table 2). Uncertainties are not estimated, because only a single NMR titration was performed for each ligand.

**Iron Coordination Chemistry.** Hydroxypyridinone ligands are especially good chelators for iron at low pH because of their relatively low  $\log K_a$  values. Acid concentrations of  $\sim 10$  M are required to liberate iron completely. For this

(44) Xu, J.; Whisenhunt, D. W., Jr.; Veeck, A. C.; Uhlir, L. C.; Raymond, K. N. *Inorg. Chem.*, manuscript submitted.

(45) Cohen, S. M.; Meyer, M.; Raymond, K. N. *J. Am. Chem. Soc.* **1998**, *120*, 6277–6286.



reason, competition methods are necessary for the determination of equilibrium constants, because iron-hydroxypyridinone complexes cannot be significantly dissociated by standard titrimetric methods. EDTA is a suitable competitor for the systems studied here because it has an iron-binding affinity of comparable strength to that of the hydroxypyridinones and accurate values are available in the literature.<sup>38,39</sup> An additional advantage is that the ferric-EDTA complex does not absorb light in the visible range (transparent above 420 nm) while the red ferric-hydroxypyridinone complexes may be conveniently monitored by their LMCT bands. A typical spectral data set is given in Figure S-3, Supporting Information. The double-peaked band shapes of the transitions are typical for iron-tris(3,2-hydroxypyridinone) complexes.<sup>11</sup>

Numerical analysis of the spectral data gave the formation constants reported in Table 2. A single protonation reaction was observed for each complex; that is, the neutral complex  $[\text{FeL}]^0$  may be protonated to give  $[\text{FeLH}]^+$ . These two species are of similar molar absorbance as illustrated for the FeTR332-Me-3,2-HOPO system in Figure S-3 of the Supporting Information. Their discrimination was made possible by the spectral decomposition performed in the course of the nonlinear least-squares refinement. The lack of spectral change is consistent with this protonation step occurring at the capping amine, remote from the chromophoric hydroxypyridinone substructures.

**Electrochemistry.** The ferric complexes were examined by square wave voltammetry at the mercury-drop electrode. This was the successful technique for the determination of aqueous redox couples of the iron complexes examined here and in a closely related study.<sup>24</sup> Use of the mercury-drop electrode was necessary because it allows application of strongly reducing (negative) potentials and no currents were observed for reduction of the ferric-hydroxypyridinone complexes at other noble-metal or glassy-carbon electrodes. The current response to the square wave voltammetric waveform is well described theoretically,<sup>25</sup> allowing reversibility to be precisely evaluated (as illustrated in Figure S-4 of the Supporting Information).

**X-ray Crystallography.** The ferric-hydroxypyridinone complexes described here are easily precipitated in the neutral, unprotonated form,  $[\text{FeL}]^0$ . X-ray diffracting crystals of this species were grown by vapor-diffusion methods. ORTEP diagrams for Fe-TREN-Me-3,2-HOPO and Fe-TRPN-Me-3,2-HOPO structures are illustrated in Figures 4 and 5, while the ORTEP diagrams for Fe-TR332-Me-3,2-HOPO and Fe-TR332-Me-3,2-HOPO structures are illustrated in Figures S-5 and S-6 of the Supporting Information. Selected bond distances and angles are given in Tables S-3, S-6, S-9, and S-12 of the Supporting Information. In each case, the expected tripodal geometry was obtained with the binding arms descending from the capping tertiary amine to encircle the hexadentate metal while the amine takes the “in” conformation with its lone electron pair pointing into

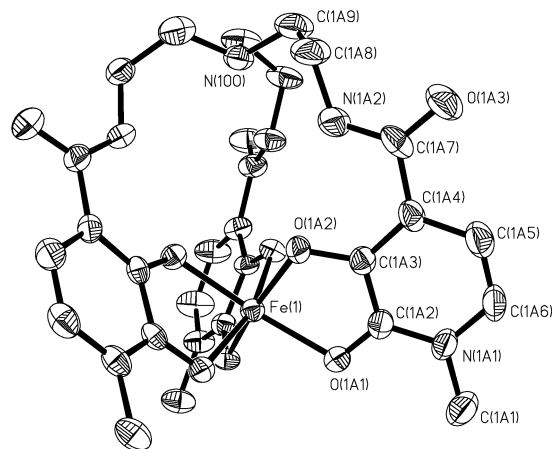


**Figure 4.** Crystal structure (ORTEP) of  $[\text{FeL}^1]\cdot\text{CH}_2\text{Cl}_2\cdot 1.5\text{C}_4\text{H}_{10}\text{O}$ . Thermal ellipsoids are drawn at the 40% probability level.

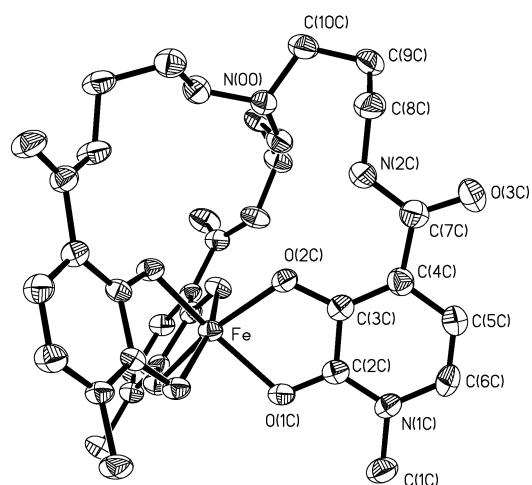


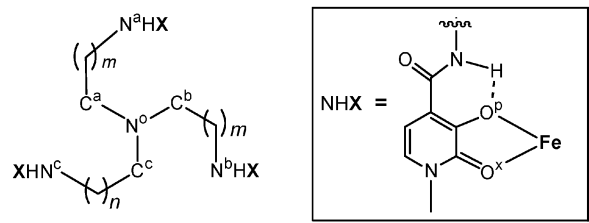
**Figure 5.** Crystal structure (ORTEP) of  $[\text{FeL}^4]\cdot\text{C}_3\text{H}_7\text{NO}\cdot\text{C}_4\text{H}_{10}\text{O}$ . Thermal ellipsoids are drawn at the 40% probability level.

the central cavity toward the metal. The “in” conformation was also observed in the crystal structure<sup>46</sup> of the similar ferric complex FeCP130.

A selection of metrical parameters for the four structures appears in Table 4. All four complexes are assigned as having pseudo-octahedral geometry based on the observed twist angles (all  $>37^\circ$ , illustrated in Figure 6.). Hydroxypyridinones differ from catecholamides by having significantly different phenolate ( $\text{O}^{\text{P}}$ ) and oxo ( $\text{O}^{\text{X}}$ ) Fe—O bond distances (difference of 0.05 Å). The FeTREN-Me-3,2-HOPO and Fe-TRPN-Me-3,2-HOPO complexes have normalized bites of 1.284 and 1.276, respectively, where the normalized bite is defined as the distance between the ligating atoms divided by the effective distance between the central metal ion and ligating atoms.<sup>47</sup> The optimum twist angle based on the lowest repulsive energy between the ligating atoms is therefore calculated as  $46.9^\circ$  and  $45.9^\circ$ , respectively.<sup>47</sup> The average twist angle of FeTREN-Me-3,2-HOPO is  $43.2^\circ$ , very close to the value of  $42.1^\circ$  for  $\text{Fe}(\text{3,2-HOPO})_3$ , an iron complex with three unsubstituted bidentate 3,2-HOPO ch-

(46) Xiao, G. Y.; Vanderhelm, D.; Hider, R. C.; Dobbin, P. S. *Inorg. Chem.* **1995**, *34*, 1268–1270.

(47) Kepert, D. L. In *Inorganic Stereochemistry*; Springer-Verlag: Berlin, 1982; pp 2–6.

**Table 4.** Metrical Parameters of the Fe–Hydroxypyridinone Complexes


		distance (Å)			
		TREN	TR322	TR332	TRPN
amide–phenol	N <sup>a</sup> –O <sup>p</sup>	2.722	2.690	2.696	2.788
	N <sup>b</sup> –O <sup>p</sup>	2.714	2.687	2.695	2.740
	N <sup>c</sup> –O <sup>p</sup>	2.698	2.666	2.678	2.711
amine–amide	N <sup>o</sup> –N <sup>a</sup>	3.061	4.172	4.113	4.306
	N <sup>o</sup> –N <sup>b</sup>	3.034	3.039	4.082	4.080
	N <sup>o</sup> –N <sup>c</sup>	3.019	2.977	3.046	3.001
amide–amide	N <sup>a</sup> –N <sup>b</sup>	4.470	5.409	5.765	6.442
	N <sup>b</sup> –N <sup>c</sup>	4.437	5.284	5.437	5.598
	N <sup>c</sup> –N <sup>a</sup>	4.401	4.504	5.250	5.498
Fe–O <sup>p/x</sup>	Fe–O <sup>p</sup>	1.989	1.980	1.985	1.992
	averages	Fe–O <sup>x</sup>	2.047	2.047	2.045

elators.<sup>48</sup> There is no capping scaffold in Fe(3,2-HOPO)<sub>3</sub>, so the identical twist angles indicate an absence of steric constraints in the TREN structure, consistent with the near perfect tetrahedral geometry at the tertiary nitrogen (average C<sup>α</sup>–N–C<sup>α</sup> angle of 109.0°, cf. 109.5° for an sp<sup>3</sup> nitrogen). The twist angle decreases slightly in the FeTR322-Me-3,2-HOPO structure (39.8°) and even more so for the FeTRPN-Me-3,2-HOPO and FeTR332-Me-3,2-HOPO structures (37.9° and 37.1° respectively), while the tertiary nitrogen–α-carbon angles flatten in these structures, illustrating the presence of small but significant steric constraints imposed by the progressively larger ligand scaffolds.

The amide nitrogen to phenolic oxygen distances (N–O<sup>p</sup>) are in all cases less than 2.8 Å, indicating the presence of strong hydrogen bonds, a characteristic feature of 4-carboxamide-3,2-HOPO ligands.<sup>5,24</sup> In addition to the amide–phenolate hydrogen bonding, there is structural evidence for weak hydrogen bonding between the amide nitrogens and the capping amine nitrogen. In each complex, there is at least one arm wherein this distance (N<sup>o</sup>–N<sup>a/b/c</sup>) is close to 3.1 Å, indicating a significant interaction. All three arms meet this criterion in the TREN-capped structure while the TRPN-cap distorts from C<sub>3</sub> symmetry so that the central amine may interact with at least one of the amide protons. This trend is consistent with the solution studies of the iron complexes in which it was found that the capping amine becomes progressively more basic (*K*<sub>a</sub><sup>FeLH</sup> becomes larger) as the cap increases.

Expansion of the internal cavity with increasing cap size is apparent in Figures 4 and 5 as well as in Figures S-5 and S-6 (Supporting Information) and is reflected in the arm-to-arm distance between each amide nitrogen of the complexes as tabulated in Table 4; these increase from an average value of 4.44 Å for the TREN-capped complex to 5.06 Å in

the TR322 case, 5.48 Å for TR332 and 5.85 Å in the case of TRPN. The amide–amide distances may be compared with those for the Fe-HOPOBactin structure.<sup>11</sup> This ligand substitutes the capping tertiary amine in the current series with the tri-lactone ring of the siderophore enterobactin which has been shown to provide a highly preorganized scaffold of near optimal size.<sup>11,12</sup> In Fe-HOPOBactin, the average amide–amide distance is 4.80 Å, intermediate between the values for the TREN- and TR322-capped complexes, suggesting these have close to the optimum cap size.

## Discussion

**Ligand Acidity.** All four of the cap-enlarged ligands examined in this study contain the same metal-binding subunit, the 4-carboxamido Me-3,2-HOPO. This exhibits a single protonation reaction which may be expected to have an intrinsic log *K*<sub>a</sub> value of ~6.1;<sup>6,7</sup> the 3 equiv of this group present in each ligand lead to the 3-proton buffer centered on pH 6 which is observed for each of the titration curves in Figure 2.

In addition to the hydroxypyridinone groups, each ligand exhibits a fourth protonation reaction due to the presence of the capping amine. Two different models may be given for this functional group. It might be expected to have a log *K*<sub>a</sub> value similar to tertiary amines such as the relatively basic tri-ethylamine, log *K*<sub>a</sub> = 10.68,<sup>49</sup> or alternatively, it may be mildly acidic as for the tris-acetyl amide of TREN (Ac<sub>3</sub>-TREN), log *K*<sub>a</sub> = 6.01 (determined here). Evidently, the TRPN-Me-3,2-HOPO ligand is closer to the first model because it displays a log *K*<sub>a</sub><sup>1</sup> value of 9.43 (Table 2), well separated from the three successive log *K*<sub>a</sub> values clustered around 6. The single-proton buffer region centered on pH 9.43 is clearly apparent in the titration curve for this ligand shown in Figure 2. As the cap is systematically reduced in size, the amine becomes progressively more acidic so that by the final ligand, TREN-Me-3,2-HOPO, a single 4-proton buffer region centered on pH 6 is observed. It appears that all four protonation sites in TREN-Me-3,2-HOPO have intrinsic (microscopic)<sup>50,51</sup> log *K*<sub>a</sub> values of ~6, leading to the observed macroscopic values which are loosely clustered around this value. We assign this increase in acidity to the stronger, 5-membered, hydrogen-bonding rings which the cap amine may form with the amide protons on the ethylene-bridged arms. The equivalent propylene-bridged arms lead to 6-membered rings and weaker amine–amide hydrogen bonding. TREN-Me-3,2-HOPO has all arms in its cap as ethylene bridges; therefore, the central amine is the most acidic in this ligand, approaching the acidity of the simplified analogue, Ac<sub>3</sub>TREN.

Further evidence appears in the pD-NMR titration data, Figure 3. The observed resonances form two distinct groups, those arising from aliphatic protons (δ = 1.5–3.8 ppm) which are sensitive to the chemical environment in the

(48) Scarrow, R. C.; Riley, P. E.; Abu-Dari, K.; White, D. L.; Raymond, K. N. *Inorg. Chem.* **1985**, *24*, 954–967.

(49) Frenna, V.; Vivona, N.; Consiglio, G.; Spinelli, D. *J. Chem. Soc., Perkin. Trans. 2* **1985**, 1865.

(50) Gergely, A.; Kiss, T.; Deak, G.; Sovago, I. *Inorg. Chim. Acta* **1980**, *56*, 35–40.

(51) Kiss, T.; Sovago, I.; Martin, R. B. *Polyhedron* **1991**, *10*, 1401–1403.

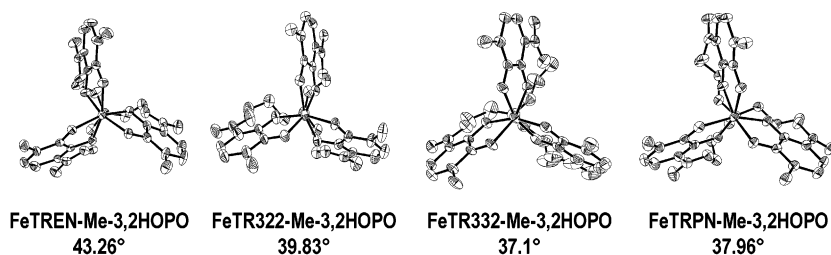


**Figure 6.** Twist angles of complexes FeTREN-Me-3,2-HOPO, FeTR322-Me-3,2-HOPO, FeTR332-Me-3,2-HOPO, FeTRPN-Me-3,2-HOPO.

capping region and those arising from aromatic protons ( $\delta = 6-7$  ppm) which act as probes for the hydroxypyridinone moieties. The ligand TRPN-Me-3,2-HOPO displays significant shifts for aromatic protons between pD 5 and 8 while aliphatic protons shift only in the pD range 8.5–10.5. Clearly, the two regions of the ligand react independently with solution protons/deuterons. Sharp contrast appears in the case for the TREN-Me-3,2-HOPO ligand wherein all resonances are simultaneously variant over the pD range 4–9. This is consistent with the findings of the previous paragraph, that each functional group has a roughly equal intrinsic acidity ( $\log K_a \sim 6$ ). Moreover, the pD-NMR data indicate that the two regions are not independent: every protonation reaction creates a substantial change in the chemical environment throughout the ligand. We suggest that a hydrogen-bonding network extends throughout the structure as described in Figure 1. In the fully protonated form,  $LH_4$ , the HOPO phenol hydroxyl is a hydrogen donor and is likely to form a 5-membered ring H-bond with adjacent HOPO-oxo group. The HOPO phenolic oxygen also serves as a hydrogen acceptor to form a 6-membered ring H-bond with the adjacent amide group. For other protonation states, the tertiary nitrogen and phenolic oxygen both become hydrogen-bond acceptors and compete for the amide proton.

**Iron Formation Constants.** On first inspection, the complex formation constants of Table 2 ( $\beta_{110}$  and  $\beta_{111}$ ) do not appear to form a regular trend with variation in ligand cap size (i.e., the values for TR332-Me-3,2-HOPO are out of sequence with those of TR322-Me-3,2-HOPO and TRPN-Me-3,2-HOPO). Systematic trends do become apparent when the values are evaluated as the parameters  $pM(Fe^{III})$  and  $K_a^{FeLH}$  [ $pM$  is the negative logarithm of free metal concentration in equilibrium with complexed and free ligand; it is analogous to the free proton concentration (pH) created by a buffer]. Calculation of this parameter provides a convenient comparison of ligands of varying acidity and/or denticity. In the present series, the  $pM$  values of Table 2 indicate that iron-complex stability increases with the number of ethylene-bridged arms in the ligands; that is, the TREN-ME-3,2-HOPO and TR322-Me-3,2-HOPO ligands form the most stable iron complexes at pH 7.4. The difference between these two ligands (i.e.,  $pM = 26.8$  and  $26.6$ ) is not significant, suggesting that a single propylene arm in the cap does not substantially decrease the stability of the complex. For comparison, it is noted that the ligand CP130 gives a  $pM$  value of 25.7,<sup>52</sup> a ferric-ion affinity at pH 7.4 equivalent to that for the TR332-capped ligand. This is consistent with the crystallographic results (discussed in a following subsec-

tion), showing that the larger scaffold and lack of amide–phenolate hydrogen bonding in CP130 gives a less optimal geometry in comparison to TREN-Me-3,2-HOPO.

The value of  $\log K_a^{FeLH}$  is calculated from the difference between the log values of  $\beta_{110}$  and  $\beta_{111}$  and represents the acidity of the protonated complex,  $[FeLH]^+$ . This protonation is assigned to the capping amine because there is such minor spectral change which accompanies protonation of the complex (Figure S-3, lower panel, Supporting Information). There is a clear increase in acidity as the cap size is reduced, from the mildly basic value of  $\log K_a^{FeLH} = 7.72$  displayed by FeTRPN-Me-3,2-HOPO to the acidic value of 3.9 displayed by FeTREN-ME-3,2-HOPO. This is consistent with the ethylene-bridged arms of the caps allowing efficient 5-membered hydrogen-bonding rings to form between the capping amine and the amide protons. The effect is more intense in the complexes than in the free ligand (i.e., the capping amines are even more acidic in the complexes) because chelation to the metal center creates a rigid structure which increases interaction between the capping amine and the amide protons.

**Electrochemistry.** All of the ferric complexes displayed reversible reduction potentials within a certain pH window presented in Table 3. This window becomes narrower and moves to higher pH with increasing cap size. Only the ferric-TREN-Me-3,2-HOPO complex may be expected to exhibit reversible reduction at physiological pH. The limits of reversibility for each complex are well predicted by the formation constants of Tables 2 and 3. At the lower (more acidic) limit, the ferrous complex is not stable with respect to proton competition while at alkaline pH the limit is determined by the point at which the ferric complex is no longer competitive with the solubility product of amorphous ferric-oxo-hydroxide ( $FeOOH(s)$ ).<sup>40</sup>

**X-ray Crystallography.** The effect of increasing scaffold size in the ferric hydroxypyridinone structures is apparent within the crystallographic structures, and the observations are consistent with the solution studies. Addition of methylene groups into the scaffold opens up the central cavity, increases the amine–amide distance within each arm of the complexes, and spreads out the arms relative to each other with increasing amide–amide distances. This is consistent with the measured acidity of the capping amine, which becomes more basic in the larger scaffolds as interactions with the amide groups decrease. The Fe-TREN-Me-3,2-

(52) Streater, M.; Taylor, P. D.; Hider, R. C.; Porter, J. *J. Med. Chem.* **1990**, *33*, 1749–1755.

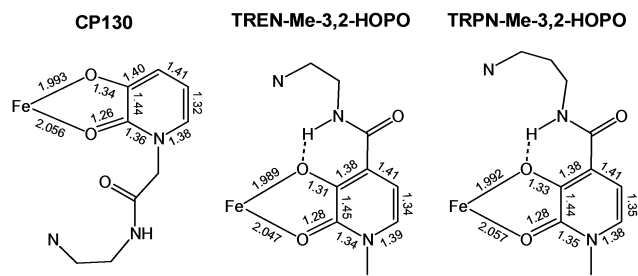


**Figure 7.** Comparison of crystal structures for the ferric complexes of CP130, TREN-Me-3,2-HOPO, and TRPN-Me-3,2-HOPO.

HOPO structure appears to have near optimal geometry while the larger scaffolds induce a small degree of steric strain as is apparent from the twist angles and the flattening out of the capping tertiary amine. This supports the solution thermodynamic studies, which found the TREN-capped ligand to exhibit the greatest stability constant for the neutral species, that is,  $\beta_{110}$  for  $[\text{FeL}]^0$ , and to have the highest affinity for ferric iron at pH 7.4 (as reflected in the pM values).

**Amide-Phenolate Hydrogen Bonding.** The crystallographic structures clearly demonstrate the hydrogen-bonding interactions between the amide groups and the proximal phenolic oxygens of the hydroxypyridinones. As noted earlier, this hydrogen bonding makes an important contribution to chelate stability<sup>3,4</sup> and has been generally observed in a wide selection of catechol-amides and similar ligands including synthetic CAM ligands,<sup>4,53</sup> natural products such as the siderophore enterobactin,<sup>54</sup> terephthalamides,<sup>4,14,55</sup> as well as hydroxypyridinones.<sup>5,24</sup>

These hydrogen bonds do not appear in the contrasting ligand design exemplified by the ligand CP130.<sup>46</sup> This ligand resembles the current series insofar as it is a hexadentate ligand based on 3,2-hydroxypyridinones, with TREN acting as the molecular scaffold. However, there is a glycine spacer between the scaffold and the attachment point on the hydroxypyridinone ring. As illustrated in Figure 7, the metrical parameters for the metal center and the hydroxypyridinone rings are almost identical with those of the structures presented here with the exception that the rings are flipped, because the ring attachment point is at the ring nitrogen rather than the 4-position. This results in a large perturbation in the scaffold geometry, with the amide groups pointing outward and being no longer able to form an internal hydrogen bond: instead, they form hydrogen bonds with the chelating carbonyl oxygens of other complexes, that is, an intermolecular bond.<sup>56</sup> In a further example, the same glycine spacer has been used to connect 3,2-hydroxypyridinone

ligands to mesitylene-based molecular scaffolds, which are not stabilized by amide–phenolate hydrogen bonding.<sup>57</sup>

## Conclusion

Preparation of the ligand series examined here was made possible by the synthesis of the benzyl-protected, thiazolide-activated 3,2-hydroxypyridinone. This convenient synthon allows the 3,2-hydroxypyridinone chelator to be attached to any primary amine. The synthesis presented here improves on previous reports and is given with greater characterization and detail. The solution chemistry of the ligands and their ferric complexes shows the strong effect of intramolecular hydrogen bonding. Crystallographic studies reveal that the expected tripodal geometry is formed by each complex and provide further evidence for intramolecular hydrogen bonding with the amide groups acting as proton donor to both the hydroxypyridinone phenolate oxygens and to the capping amine. The TREN-capped ligand appears to provide a near-optimal geometry for ferric-iron binding; its central amine is the most acidic in the free and complexed forms. This ligand is also the strongest iron chelator, a fortuitous result because TREN is the most readily available of the capping amines. Each of the ferric-chelates may be reversibly reduced to the ferrous form in aqueous media. This reaction occurs within a pH window which is well predicted by the equilibrium constants. The hydroxypyridinone ligands presented here are powerful chelators of ferric iron, forming complexes with relatively negative reduction potentials. The chemistry presented here augments the biological studies (in vitro and in vivo) which have shown the promise of TREN-Me-3,2-HOPO as an iron sequestering agent.

**Acknowledgment.** We thank Dr. Donald W. Whisenhunt, Jr., for the initial surveys of ferric-TREN-Me-3,2-HOPO coordination chemistry, Dr. Michel Meyer for assembling the pD titrations, Dr. Oleg Aleksiuik for help with the NOE data, and Drs. Paul Walton and F. J. Hollander for assistance with the X-ray diffraction studies. This research was supported by NIH Grants DK 32999 and DK 57814.

**Supporting Information Available:** Tables of crystallographic solution data, atomic coordinates and displacement parameters, bond distances and angles, and formation constants. Figures showing solution speciation, NOE spectra, voltammograms, and ORTEP diagrams. X-ray crystallographic files for  $\text{FeTREN-Me-3,2-HOPO} \cdot 0.375\text{C}_4\text{H}_{10}\text{O} \cdot 0.5\text{CH}_2\text{Cl}_2$ ,  $\text{FeTR322-Me-3,2-HOPO} \cdot \text{CHCl}_3 \cdot \text{CH}_3\text{OH} \cdot 0.5\text{C}_6\text{H}_{14} \cdot 0.5\text{H}_2\text{O}$ ,  $\text{FeTR332-Me-3,2-HOPO} \cdot 3.5\text{CH}_3\text{OH}$ , and  $\text{FeTRPN-Me-3,2-HOPO} \cdot \text{C}_3\text{H}_7\text{NO} \cdot \text{C}_4\text{H}_{10}\text{O}$  in CIF format. This material is available free of charge via the Internet at <http://pubs.acs.org>.

IC025610+

(53) Stack, T. D. P.; Karpishin, T. B.; Raymond, K. N. *J. Am. Chem. Soc.* **1992**, *114*, 1512–1514.

(54) Karpishin, T. B.; Raymond, K. N. *Angew. Chem., Int. Ed. Engl.* **1992**, *31*, 466–468.

(55) Xu, J.; Stack, T. D. P.; Raymond, K. N. *Inorg. Chem.* **1992**, *31*, 4903–4905.

(56) Xiao, G. Y.; Vanderhelm, D.; Hider, R. C.; Rai, B. L. *J. Phys. Chem.* **1996**, *100*, 2345–2352.

(57) Rai, B. L.; Khodr, H.; Hider, R. C. *Tetrahedron* **1999**, *55*, 1129–1142.